

Trapped-hole centers in neutron-irradiated synthetic quartz

C. B. Azzoni

Dipartimento di Fisica "A. Volta" dell'Universita' di Pavia, via Bassi 6, I-27100 Pavia, Italy

F. Meinardi and A. Paleari

Dipartimento di Fisica dell'Universita' di Milano, via Celoria 16, I-20133 Milano, Italy

(Received 1 June 1993; revised manuscript received 23 November 1993)

EPR signals of two defect centers in neutron-irradiated high-purity quartz have been analyzed. The principal values and the anisotropy of the g tensors suggest an attribution to peroxy radicals and non-bridging oxygen hole centers.

In amorphous silica, radiation-induced paramagnetic hole centers have been extensively studied and three types of intrinsic hole defect may be distinguished: (i) the "nonbridging-oxygen hole center" (NBOHC),^{1,2} (ii) the "peroxy radical" (PR),^{1,2} and (iii) the "self-trapped hole" (STH).^{3,4} For these paramagnetic centers, models have been inferred by comparing the experimental g values with those calculated for similar defects,^{5,6} and by analyzing the hyperfine structure (hfs) due to ¹⁷O and ²⁹Si in isotopically enriched material.

By contrast, electron-paramagnetic-resonance (EPR) signals of intrinsic hole centers have never been identified in crystalline quartz:⁷ probably, as regards STH's in regular sites of the crystalline lattice, the fast hopping rate of holes between pairwise equivalent oxygen atoms precludes the detection of their EPR signal at temperature higher than a few kelvins.⁸ On the other hand, trapped-hole centers at intrinsic structural defects, in configurations similar to the NBOHC's or PR's observed in amorphous silica, should be easily detected; the failure in creating them in quartz by purely ionizing radiation shows an apparent lack in quartz of the relevant number of intrinsic defect precursors, like nonbridging oxygen atoms or peroxy linkages, otherwise easily stabilized in the disordered structure of silica. As a matter of fact the observed trapped holes in quartz are generally confined at impurities,⁷ giving rise to the EPR signals of the well-known aluminum hole centers (AlHC's),⁹⁻¹¹ germanium hole centers (GeHC's),⁸ hydrogen hole centers,¹² and other less defined impurity hole centers.¹³⁻¹⁶

Nevertheless, particle irradiation may induce defects also by atomic displacement, and is expected to create in quartz the molecular species which can trap holes in configurations analogous to the silica PR and NBOHC. A group of lines, accompanying the narrow E' resonance in the EPR spectrum of fast-neutron-irradiated quartz, was tentatively associated with intrinsic hole defects by Weeks in 1956,¹⁷ but a detailed analysis of the signals was not achieved. The E' resonances were further studied both in quartz and in silica by many other authors, giving detailed models for the different variants of the defect responsible, while the holelike EPR lines were almost ignored, perhaps because this complex of signals, often overlapped with other signals, is difficult to induce in

pure quartz, requiring displacing irradiation. Furthermore, more studies have been devoted to the identification of EPR centers in silica than in quartz, as interest grew in the amorphous form of SiO₂. Therefore, no definite evidence of intrinsic hole centers in crystalline SiO₂ has been reported in the literature to our knowledge since the early observation of Weeks, except an EPR signal in natural quartz attributed to an unpaired spin at a peroxy linkage¹⁸ with g values very different from those observed in silica for analogous defects. Anyway, no data concerning the environment and compatibility of PR's and NBOHC's with the crystalline lattice of quartz have been available, up to now. In this framework, we have carried out an EPR study of neutron-irradiated high-purity quartz in the spectral region of the E' center and of the PR's and NBOHC's observed in silica.

Single crystals of Sawyer PQ quartz were cut in bars and exposed in a reactor to neutron fluences ranging from 10^{17} to 10^{18} neutrons cm⁻², with about 70% of the beam constituted by thermal neutrons; the irradiation treatments, at temperature lower than 100°C, have been chosen to be intense enough to create the relevant number of paramagnetic defects but sufficiently weak to avoid amorphization of the lattice.¹⁷ EPR measurements have been performed in the X band (about 9.13 GHz) between 120 K and room temperature, at microwave powers ranging from 10^{-5} to 10^{-1} W. The lines arising from different centers, each present in six equivalent orientations in the crystalline lattice, have been identified and grouped by considering the dependence of linewidth and intensity on temperature, microwave power, and neutron fluence. The anisotropy of the EPR spectrum has been studied by rotating the crystal in the magnetic field. In Fig. 1 typical experimental spectra are shown for two different crystal orientations, at high microwave power and at room temperature.

Among the numerous lines of the spectrum, we have identified, besides the E' -center signal, two signals in the typical spectral region of hole centers. These signals are relatively weak with respect to other intense lines (whose attributions are still lacking), but their strong anisotropy has allowed us to discriminate them among the other overlapped signals. When the magnetic field is directed along the z axis of the crystal, the two signals consist only

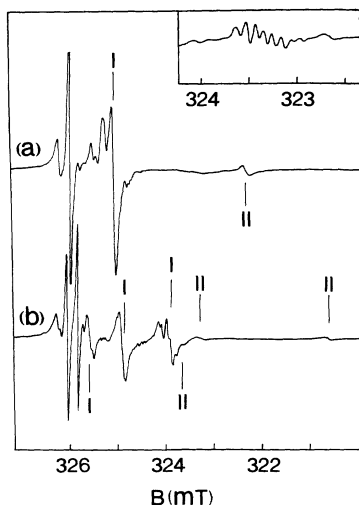


FIG. 1. Typical first-derivative EPR spectra of neutron-irradiated quartz (4×10^{17} neutrons cm^{-2}) detected at 300 K with the magnetic field B in the yz plane and the angle $\angle Bz$ equal to (a) 0° and (b) 18° . In the inset, a restricted spectral region is shown in an experimental configuration ($\angle Bz = 54^\circ$, $T = 200$ K) which clearly evidences the hf structure of signal I.

of two components at $g_z = 2.0076$ and $g_z = 2.0250$ (signals I and II in Fig. 1, respectively). The spectral position and anisotropy of the signal II do not correspond to those of any other signal reported in the literature, while signal I shows several similarities with the signals of the undefined centers D and E identified in natural quartz by Maschmeyer and Lehmann.¹³

Signals I and II show g values larger than that of the free electron, well-defined anisotropy, and low microwave saturation. Besides, signal I exhibits a hyperfine structure (see the inset in Fig. 1) arising from a very weak hyperfine interaction (with a hf coupling constant of about 0.06 mT), anisotropic, with a 100% abundant nuclear spin with $I > \frac{1}{2}$. A detailed analysis of the anisotropy of the hf splitting has not been achieved because it is precluded by the overlap of other neutron-induced resonances. Signal II is the weaker one and does not show any hyperfine structure over the noise.

Figure 2 summarizes the data obtained by rotating the magnetic-field direction in the yz plane of the crystal (the mean positions of the hfs of signal I are reported). In the same figure, the continuous lines are the fits obtained by using as free parameters the principal values of the g tensor and the angles between the magnetic-field direction and the defect axis.

The calculated parameters are reported in Table I: the polar and azimuthal angles ϑ and ϕ , measured from the z and x crystal axis, respectively, correspond to one of six equivalent sites, the directions of the other five sites being $(\vartheta, \phi \mp 120^\circ)$, $(180^\circ - \vartheta, -\phi)$, and $(180^\circ - \vartheta, -\phi \mp 120^\circ)$. We use a right-handed orthogonal coordinate system with the z axis parallel to the c axis and the x axis parallel to a twofold crystal axis. Table II shows the g values of some representative hole centers observed in quartz and in silica.

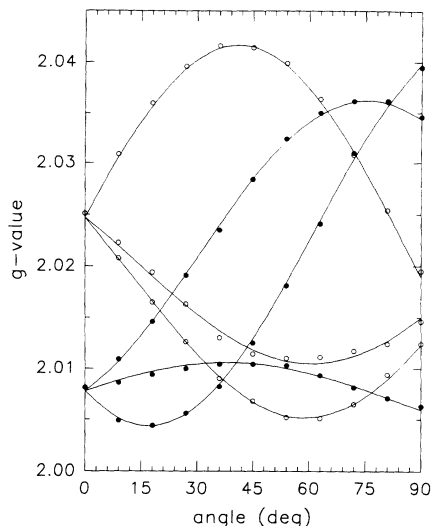


FIG. 2. Angular dependence of the spectral positions of the EPR signals I (●) and II (○) when the magnetic field is rotated in the yz plane of the crystal. Solid lines are generated from the parameters of Table I.

We will discuss the results starting from a comparison between the values of Tables I and II. The principal g values of the signals I and II (see Table I) match well with those of some typical hole centers observed in quartz: the AlOHC, the GeOHC (see Table II), and their variants.^{8,10,11} The g values of signals I and II also agree with the principal g values of the intrinsic oxygen-hole centers observed in silica (PR, NBOHC, and STH in Table II). But, as regards the AlOHC and the GeOHC, the directions of the principal axes are different from those observed for the signals I and II: in one AlOHC and the GeOHC, the axis characterized by the largest g shift is nearly parallel to a Si-Si direction, as expected⁹ in M - \dot{O} - M defect structures (where M is a silicon or a substitutional cation impurity, and \dot{O} is a bridging oxygen with a trapped hole in a lone-pair orbital perpendicular to the plane defined by the M - O - M bonds). By contrast, none of the g -tensor components in Table I is aligned along a Si-Si direction. Also, attribution to a STH in a regular site of the lattice is to be ruled out, because the STH should consist of a hole trapped in a lone-pair orbital of a bridging oxygen,³ with the same symmetry as the AlOHC and GeOHC in quartz. We also note that the largest g -shift directions in Table I deviate from the

TABLE I. Calculated parameters of signals I and II.

Signal	g principal values	Polar angle ϑ (deg)	Azimuthal angle ϕ (deg)
I	2.0503	75.77	244.75
	2.0081	136.83	170.43
	2.0026	50.32	142.61
II	2.0417	40.82	211.75
	2.0125	129.70	195.70
	2.0011	82.01	112.40

TABLE II. g values of some representative hole centers.

Signal	g principal values	Material	Polar angle ϑ (deg)	Azimuthal angle ϕ (deg)
AlOHC	2.0602	quartz ^a	119.25	57.62
	2.0085		124.43	305.05
	2.0020		131.65	177.49
GeOHC	2.046	quartz ^b	122.2	53.6
	2.008		124.9	297.6
	2.003		128.6	173.8
NBOHC	2.078	silica ^c		
	2.0095			
	2.000			
PR	2.067	silica ^c		
	2.0078			
	2.0018			
STH	2.049	silica ^d		
	2.0093			
	2.0026			

^aReference 10.^bReference 8.^cReference 1.^dReference 3.

O—O crystal directions, thus excluding attribution to holes shared by two bridging oxygens in regular sites of the lattice (as in the case of the defect described by Baker and Robinson¹⁸ and in the tentative interpretation of the signals D and E of Maschmeyer and Lehmann¹⁵).

In summary, comparison of the principal g values in Table I with those of other defects in quartz and silica strongly suggests that the signals I and II may arise from holes trapped in oxygen sites O^- or O_2^- , but, as one may argue from the observed principal axis, the possible defect models should not involve oxygens in the bridging configurations $M-O-M$ or $M-O-O-M$. Thus, it is likely that the responsible defects (probably O^- or O_2^- species) are incorporated in quartz as dangling radicals (NBOHC's and PR's), as already observed in amorphous silica.²

In order to test the possible association of the signals I and II with PR- and NBOHC-like defects, we will consider once more the principal g values in Tables I and II, particularly the g_2 and g_3 components of the g tensor: comparison between our data and those of the silica defects in Table II is perhaps more reliable for these components since the g_1 value reported for PR's and NBOHC's in silica is calculated from broad distributions of g values used to fit powder signals.¹ We have already noted that the g_2 and g_3 values of the PR and NBOHC signals are quite similar to those of signals I and II, respectively; moreover, there is a noteworthy correspondence between the ($g_2 - g_3$) values: the signal I is as much less orthorhombic than signal II as is the PR signal compared with the NBOHC signal. On the basis of these correspondences, one may preliminarily associate signal I with PR-like defects and signal II with NBOHC-like defects.

Indications which may support this attribution may be derived by comparing the experimental principal direc-

tions of Table I with those expected from theoretical models: an analysis of the electronic levels of PR and NBOHC defects^{5,6} shows that, for PR's, the g_1 axis is parallel to the O—O bond and the g_3 axis is normal to the M -O—O plane, while, for NBOHC's, the g_1 axis is along a Si—O direction; in both cases, the direction of g_3 must be orthogonal to a Si—O bond of the crystal lattice.

As regards signal I, we have found that the experimental direction of g_3 is nearly orthogonal to the "short" Si—O bond directions of the perfect lattice,¹⁹ the angle being about 87°. This result is consistent with both PR and NBOHC models, but the attribution to a NBHOC should be ruled out because the g_1 axis deviates more than 10° from any Si—O direction. By ascribing the g_1 direction of the signal I to the direction of the O—O bond of a PR-like defect, the angle M -O—O turns out to be 169°: this agrees with the fact that a deviation from 180° is required in order that an EPR signal be detected.⁶ On the other hand, the resulting structure is not too far from the case of a linear molecule, so as to be consistent with the theoretical model¹⁵ which well reproduces the experimental g values but only in perturbative approximation with respect to the linear radical. We note that the angle deduced from our experimental data deviates from the value of 136° estimated by Edwards and Fowler²⁰ by minimizing the energy of the defect site by means of molecular-orbital methods. But they did not take into account neighboring impurities which, as we will discuss below, appear to be crucial in quartz for the stabilization of the defect.

Considering signal II, tentatively attributed to NBOHC centers, the analysis of the direction of the calculated defect axis shows that the signal anisotropy is consistent with the structure of a NBOHC defect: according to what is reported above for NBOHC's,^{2,6} signal II seems to satisfy the conditions that the g_1 direction is nearly parallel to a Si—O bond (3.44° from the long Si—O bond). By following this association, the g_3 direction, which is orthogonal to the Si—O bonds, corresponds to that of the p -like orbital which contains the hole responsible for the EPR signal, and lies in the plane defined by the Si—O—Si directions.

Now we consider the observed hfs of signal I. Since it is not accompanied by an unsplit central line, it arises from interactions with 100% abundant nuclei; by comparing the density of neutron-induced EPR centers with the impurity content, the possible candidates turn out to be ¹H and ²⁷Al. Owing to the great number of hf lines, it is likely that the hfs is due to ²⁷Al nuclei. But the small value of the hf coupling constant, about 0.06 mT, suggests that the aluminum does not enter directly into any molecular orbitals of the defect, and that the local configuration of the EPR center should be of the Si—O—O type rather than an Al—O—O defect (AlPR): an AlPR should have a signal with a hf splitting ten times larger than that observed, as we may derive from the hf splitting due to ²⁹Si of the PR detected in ²⁹Si-enriched silica,² since ²⁷Al and ²⁹Si should give rise in this case to comparable hf interaction.² The strong anisotropy of the hf splitting agrees with this picture, since it indicates that anisotropic dipolar interactions prevail over contact interactions, and the overlap of the electronic orbital at the

$I = \frac{5}{2}$ nucleus should be small. Nevertheless, the presence of aluminum, probably in the neighboring structural tetrahedra, must be crucial for the stabilization of the center: there is no variant of this EPR signal without the observed hfs. As regards signal II, its weak intensity does not allow any evidence of hfs, namely, the hfs due to the 4.7% abundant ^{29}Si , which should be bound to the non-bridging oxygen.

In summary, we report EPR signals whose spectro-

scopic features, compared with those of other EPR centers in quartz and silica as well as with theoretical models, suggest that the responsible defects may be the quartz variants of the PR and NBOHC, defects previously observed only in silica.

It is our pleasure to thank Professor Tazio Pinelli for his useful advice and for valuable discussions of the neutron damage processes.

-
- ¹M. Stapelbroek, D. L. Griscom, E. J. Friebele, G. H. Sigel, Jr., *J. Non-Cryst. Solids* **32**, 313 (1979).
²D. L. Griscom and E. J. Friebele, *Phys. Rev. B* **24**, 4896 (1981).
³D. L. Griscom, *Phys. Rev. B* **40**, 4224 (1989).
⁴P. V. Chernov, E. M. Dianov, V. N. Karpechev, L. S. Kornienko, I. O. Morozova, A. O. Rybaltovskii, V. O. Sokolov, and V. B. Sulimov, *Phys. Status Solidi B* **155**, 663 (1989).
⁵H. R. Zeller and W. Känzig, *Helv. Phys. Acta* **40**, 845 (1967).
⁶R. A. Weeks, in *Interaction of Radiation with Solids*, edited by A. Bishay (Plenum, New York, 1967), p. 55.
⁷J. A. Weil, *Phys. Chem. Miner.* **10**, 149 (1984).
⁸W. Hayes and T. J. L. Jenkin, *J. Phys. C* **19**, 6211 (1986).
⁹M. C. M. O'Brien, *Proc. R. Soc. London, Ser. A* **231**, 404 (1955).
¹⁰R. H. D. Nuttal and J. A. Weil, *Can. J. Phys.* **59**, 1696 (1981).
¹¹J. H. Mackey, Jr., *J. Chem. Phys.* **39**, 74 (1963).
¹²R. H. D. Nuttal and J. A. Weil, *Solid State Commun.* **33**, 99 (1980).
¹³D. Maschmeyer and G. Lehmann, *Z. Kristallogr.* **163**, 181 (1983).
¹⁴A. B. Vassilikou-Dova, K. Eftaxias, and G. Lehmann, *Z. Naturforsch. Teil A* **44**, 278 (1989).
¹⁵D. Maschmeyer and G. Lehmann, *Phys. Chem. Miner.* **10**, 84 (1983).
¹⁶M. I. Samoilovich, A. I. Novozhilov, L. I. Tsinober, and A. G. Malyshev, *J. Struct. Chem.* **14**, 416 (1973).
¹⁷R. A. Weeks, *J. Appl. Phys.* **27**, 1376 (1956).
¹⁸J. M. Baker and P. T. Robinson, *Solid State Commun.* **48**, 551 (1983).
¹⁹Y. Le Page and G. Donnay, *Acta Crystallogr. Sect. B* **32**, 2456 (1976).
²⁰A. H. Edwards and W. B. Fowler, *Phys. Rev. B* **26**, 6649 (1982).